PCCP

View Online
Dynamic Article Links

Cite this: DOI: 10.1039/c0cp02435j

www.rsc.org/pccp

PAPER

Polarization and temperature dependent spectra of poly(3-hydroxyalkanoate)s measured at terahertz frequencies

Hiromichi Hoshina,*[a] Yusuke Morisawa,[b] Harumi Sato,[b] Hiroaki Minamide,[a] Isao Noda,[c] Yukihiro Ozaki[b] and Chiko Otani[a]

Received 6th November 2010, Accepted 25th February 2011
DOI: 10.1039/c0cp02435j

Temperature-dependent terahertz (THz) absorption spectra of poly(3-hydroxyalkanoate)s (PHAs) were measured by using a Fourier transform far-infrared (FT-FIR) spectrometer and a THz time-domain spectrometer over a temperature range of 10 K to 465 K with a liquid helium cryostat and a heating cell. Clear differences were observed between the spectra of crystalline and amorphous polyhydroxybutyrate (PHB), indicating that the absorption peaks observed in the THz spectra originated in the higher-order conformation of PHB. The polarization spectra of a stretched PHB sample were measured, and the direction of the vibrational transition moment was determined. The temperature dependences of the spectra reveal frequency shifts and broadening of the absorption peaks with temperature, suggesting large anharmonicity of the vibrational potential. The temperature shift behaviour is quite different in each transition. Some of the transitions show a blue shift, which cannot be explained by a simple anharmonic potential model. Frequency shifts of the peaks were mainly observed below 10 THz, which suggests a large anharmonicity of the vibrational potential at lower frequencies.

Introduction

Despite a long history dating back to the 1950s,[1] vast unexplored fields remain in molecular spectroscopy in the terahertz (THz) frequency region. Spectrometers have not been sensitive enough to measure the spectra of optically thick samples with a good signal-to-noise ratio. The development of Fourier transform infrared spectrometry (FT-IR) in the 1980s has made measurement in the far infrared much easier.[2] Some difficulty still remains for measurement at frequencies lower than 100 cm^{-1} (= 3 THz), because the Si bolometer used as a detector in this frequency region must be cooled by liquid helium. Measurement of THz spectra has recently become easier with the development of the terahertz time-domain spectroscopy (THz-TDS) technique.[3,4] Since THz-TDS detects the THz electric field coherently, the signal is free from thermal background noise, and the obtained spectra show a quite high dynamic range in the frequency region below 3 THz.[4,5] As a result, many applications using characteristic spectra in the THz frequency range (so-called fingerprint spectra) have become possible, such as detection of illicit drugs,[6,7] detection of explosives,[8,9] and imaging of cultural heritages.[10] Most of those applications use fingerprint spectra of organic molecules to identify materials.[11,12]

However, the assignment of the THz fingerprint spectra itself is still in its infancy. Since low-frequency vibrational modes originate from intramolecular vibrational motions coupled with intermolecular motions, their vibrational frequencies change dramatically with the development of crystal structure.[13] Moreover, the anharmonicity of the potential and large amplitude of vibrational motion make *ab initio* calculations difficult. Jepsen and Clark have succeeded in assigning THz spectra of sucrose by density functional theory (DFT) calculation in consideration of its crystal structure.[14] Recently, King *et al.* investigated the anharmonicity of lattice vibrations in hydrated molecular crystals.[15] However, in many cases, the origin of THz spectra is not clearly understood. Additional spectroscopic evidence, such as polarization spectra that determine the orientation of vibrational dipole moments, may also facilitate the assignment. In our previous work, we found that THz absorption spectra of poly(3-hydroxyalkanoate)s (PHAs) show clear peaks originating from the higher-order conformation of a polymer chain.[16] By using polarization spectra of stretched poly(3-hydroxybutyrate) (PHB), in which the *c*-axis of the lamellar crystal is aligned, we successfully revealed the orientation of the vibrational dipole moments. The polarization and temperature dependence of the spectra of PHB may yield detailed information about vibrational motions in crystalline PHB.

[a] *RIKEN, 519-1399 Aramaki-Aoba, Aoba-ku, Sendai, Miyagi 980-0845, Japan. E-mail: hoshina@riken.jp*
[b] *Department of Chemistry, School of Science and Technology, Kwansei Gakuin University, Gakuen, Sanda, Hyougo 669-1337, Japan*
[c] *The Procter & Gamble Company, 8611 Beckett Road, West Chester, Ohio 45069, USA*

Far infrared spectroscopy of polymers has been studied since the 1970s.[17] In many cases, polymers show broad absorption features in the far infrared due to skeletal motions of a polymer chain and librational motions of side groups. Wietzke *et al*. recently studied temperature-dependent spectra of high-density polyethylene[18,19] and polyvinylidene[19] by using THz-TDS. They observed that the thermal gradient of crystal lattice modes changes at the glass transition temperature, which indicates a strong interaction between the amorphous and crystalline domains in the polymer. Vibrational peaks due to hydrogen bonds are known to be observed at lower frequencies. Such peaks are observed in the THz spectra of polymers having hydrogen bonds, such as nylon,[20] poly-(methacrylic acid),[21] poly(lactic acid),[22] and PHB.[16] By using THz spectroscopy, we may obtain detailed information about how hydrogen bonding results in the higher-order conformation of polymers.

In the present study, we measured absorption spectra of PHB in a wider frequency range and a wider temperature range than in the previous study. We used both FT-FIR and THz-TDS to obtain spectra in the frequency region from 1 to 19 THz. By expanding the frequency range, we may be able to observe differences between global vibrational motions at lower frequencies and local vibrational motions at higher frequencies. Temperature-dependent THz spectra of PHB were obtained between 10 K and 440 K. With decreasing temperature, the linewidths of vibrational peaks are reduced, and overlapping bands may be separated.[23] Also, the frequency shift of the peak position indicates the anharmonicity of the vibrational potentials. Polarization spectra, which provide information on the vibrational dipole transition moments of separated peaks, were measured at 10 K and will facilitate the assignment of THz spectra of PHB.

PHAs have received keen interest for their potential as a biodegradable plastic.[24–29] Their physical properties have been a subject of active research. Fig. 1(a) and (b) show the chemical structure of PHB and poly(3-hydroxybutyrate-*co*-3-hydroxyhexanoate) (P[HB-*co*-HHx]), respectively. Fig. 1(c) and (d) show schematic figures of the molecular structure of the amorphous and crystalline phases, respectively, which were obtained by X-ray diffraction measurement.[30] In the amorphous phase, molecular chains tangle randomly. In the crystalline phase, molecular chains make up a lamellar crystal in which helical structures are aligned along the *c*-axis.[30] The dashed lines in Fig. 1(c) and (d) depict the hydrogen bonds between the C═O group and the CH_3 group. Previous infrared and X-ray diffraction studies by Sato *et al*. revealed that the direction of the hydrogen bonds in the lamellar crystal is parallel to the *a*-axis.[31–33] X-Ray diffraction measurement has shown that the amount of amorphous content increases in the P(HB-*co*-HHx) copolymer, and the thickness of its lamellar structure decreases. This change occurs because the replacement of CH_3 units with C_3H_7 units hinders the periodical folding of the polymer chain.[28] The crystallinity of PHB homopolymer is about 55%, and that of P(HB-*co*-HHx) (HHx = 12 mol%) is about 30–40%.[25] Recently, Sato *et al*. studied PHAs by infrared spectroscopy,[31,32,34,35] Raman spectroscopy,[35] near-infrared spectroscopy,[36] X-ray diffraction measurement,[32,34,37] and differential scanning calorimetry (DSC) measurement[34] and demonstrated the contribution of C═O···H–C hydrogen bonding between two helices to the crystal morphology. THz spectroscopy may also provide new insight into the relationship between hydrogen bonding and the higher-order conformation, which directly reflects the physical properties of PHAs.

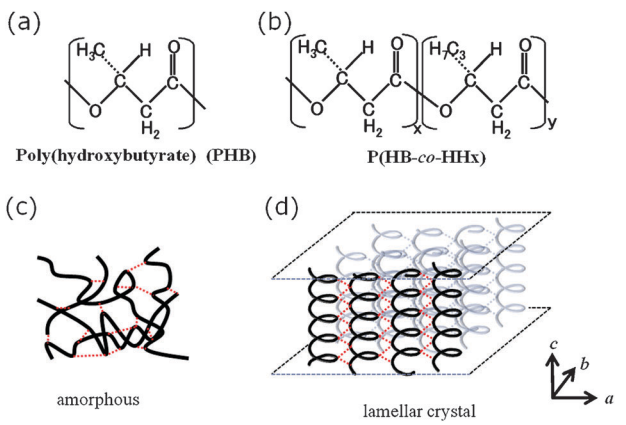

Fig. 1 Chemical structures of (a) PHB and (b) P(HB-*co*-HHx) and schematic diagrams of their molecular structures in the (c) amorphous and (d) lamellar crystal states.

Experimental

Sample preparation

Four different types of PHA samples, isotactic PHB homopolymer (Aldrich Corp.), synthetic amorphous atactic PHB (Procter & Gamble Co.), P(HB-*co*-HHx) with an HHx content of 12% (Procter & Gamble Co.), and highly stretched PHB (donated by Prof. Tadahisa Iwata) were prepared as follows. Isotactic PHB and P(HB-*co*-HHx) powder were melted at 185 °C, pressed (below 0.5 N mm^{-2}), and then slowly cooled to 40 °C in two hours and formed into a film about 100 μm thick. Amorphous PHB was spread directly onto a polypropylene window with a thickness of 2 mm to measure its spectrum, because it is a viscous liquid at room temperature. Highly stretched PHB was prepared by the following procedure. A sheet of PHB was drawn up to 1000% at 165 °C and annealed for two hours at 100 °C. Under such stretching conditions, the *c*-axis of the lamellar crystal aligns in the stretched direction.[29] Note that the moisture content of PHB is surprisingly low compared to many other types of polyester. We estimated the moisture content of PHB to be no more than 200 to 600 ppm for typical resin samples.

Terahertz and FIR spectra

The absorption spectra of the PHAs were measured by conventional THz-TDS (Aispec: *pulse* IRS-2300) and FT-FIR (ABB Bomem Inc.: DA8) spectrometers. THz-TDS was used for the measurements between 0.3 and 4.0 THz. A THz single-cycle pulse was generated and detected by a dipole-type GaAs photo-conductive antenna,[4] which was pumped by a Ti–Sapphire mode-locked laser (FEMTOLASERS: FUSION™). The waveform of the THz electric field was recorded as a function of time, and power spectra were obtained by Fourier

transformation of the THz electric field waveform. The frequency resolution of the spectra was 0.03 THz.

An FT-FIR spectrometer was used for measurements in the wider frequency region from 1 THz to 20 THz with a frequency resolution of 0.06 THz. A combination of a high-pressure mercury lamp as a THz light source, a Mylar™ film as a beam splitter, and a deuterated triglycine sulfate (DTGS) or Si bolometer as a detector was used.

The samples were placed in a vacuum chamber, which was pumped below 1 Pa to reduce the absorption of water vapour. For each measurement, spectra of both a sample and a reference were measured. The absorbance $\alpha(\nu)$ was obtained by the equation $\alpha(\nu) = -\mathrm{Log}_{10}\left(I_s/I_r\right)$, where I_s is the power spectrum of a sample, and I_r is that without the sample. The polarization spectra were measured by using a wire-grid polarizer (40 lines mm^{-1}, Specac Inc.), which was placed between the light source and the FT-FIR sample. The polarization dependence of the spectra was measured by rotating a polarizer.

The temperature of the PHA samples was changed by a heating cell and a liquid-helium-cooled cryostat (Oxford Instruments: Cryojet). Spectra at 300 K to 440 K were measured by holding a PHA film in the centre of an aluminium cell (30 mm × 30 mm × 30 mm) which was heated by an electric heater. The temperature of the heating cell was monitored by a platinum resistance thermometer. Spectra at 10 K to 300 K were measured by using the cryostat. The temperature of a sample was changed by controlling the flow rate of liquid helium and the heater attached to the sample holder.

Results and discussion

THz spectra of three types of PHA

Fig. 2 shows absorption spectra of PHB (10 K), P(HB-*co*-HHx) (10 K), and amorphous PHB (28 K) measured by FT-FIR. The absorbances of PHB and P(HB-*co*-HHx) were normalized by the sample thickness measured by a micrometer. The absorbance of amorphous PHB is shown in arbitrary units. The spectrum of PHB shows sharp peaks, with a linewidth of about 0.15 THz (FWHM). In contrast, a peak was barely observed in the spectrum of amorphous PHB, and a broad absorption feature appears from 1 to 8 THz. The differences between these two spectra reveal that the sharp absorption peaks in the spectra of PHB are due to the vibrational motions of the lamellar crystal.

The spectrum of P(HB-*co*-HHx) is similar to that of PHB, but features appear that are somewhat intermediate between the spectra of PHB and of amorphous PHB. First, the intensity of the peaks decreases by approximately 60% in the spectrum of P(HB-*co*-HHx) compared with that of PHB, which is in good agreement with the ratio of crystallinity between PHB (65%) and P(HB-*co*-HHx) (30–40%).[25] The baseline of the spectrum of P(HB-*co*-HHx) is higher than that of PHB and gradually increases between 6 and 8 THz. The increase of the baseline is due to the amorphous phase in the sample.

The linewidths of P(HB-*co*-HHx) are broader than those of PHB. Since the vibrational potential of molecules close to the surface of a crystal is different from that of molecules inside the crystal, the smaller lamellar size and defects in the crystal

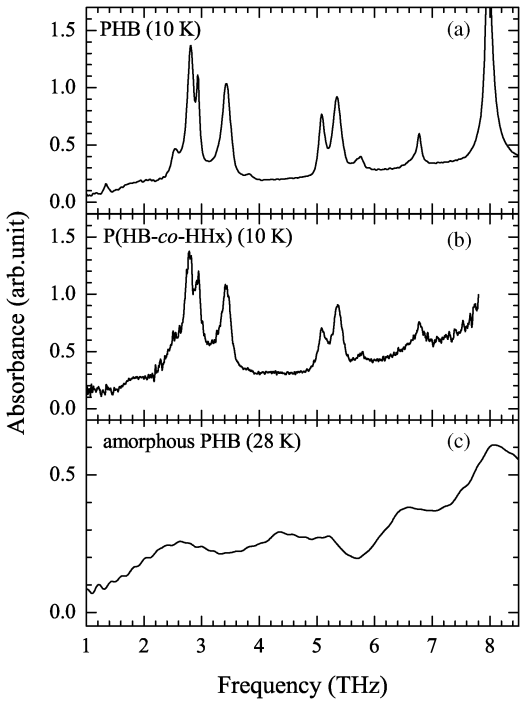

Fig. 2 THz absorption spectra of three different types of PHA measured by FT-FIR: (a) PHB measured at 10 K, (b) P(HB-*co*-HHx) measured at 10 K, and (c) amorphous atactic PHB measured at 28 K.

structure of P(HB-*co*-HHx) increase the inhomogeneous broadening of the vibrational transitions. In the spectrum of P(HB-*co*-HHx), vibrational bands at 1.8 and 2.5 THz show broader linewidths than the other bands. The vibrational modes of those two transitions are more sensitive to the size and defects of the crystal structure.

The thickness of the lamellar crystal of PHB is about 5.3 nm, and that of P(HB-*co*-HHx) is about 1.9 nm.[28,33] If the observed transitions are global vibrational motions like phonon modes in the crystal, frequency shifts must be observed between the spectra of PHB and P(HB-*co*-HHx). However, most of the PHB and P(HB-*co*-HHx) peaks are observed at almost the same frequencies in the spectra of Fig. 2. Differences appear only at frequencies below 2 THz. In the spectrum of P(HB-*co*-HHx), the peak at 1.34 THz was not observed. Instead, a broad absorption feature was observed at 1.8 THz. The differences between these two spectra suggest that the vibrational motion of this band represents global modes, which are sensitive to the size of the lamellar crystal.

Polarization spectra of PHB

Since low-frequency vibrational motions originate in intra-molecular motions strongly coupled with intermolecular motions, the assignment of the observed peaks in Fig. 2 is not a simple task. Theoretical calculations treating the crystal structure with a precise intermolecular potential are necessary for the assignment of THz spectra. Polarization spectra may help, because the direction of a vibrational dipole moment relative to the *c*-axis of the crystal is obtained by the intensity ratio between parallel and perpendicular polarization spectra.

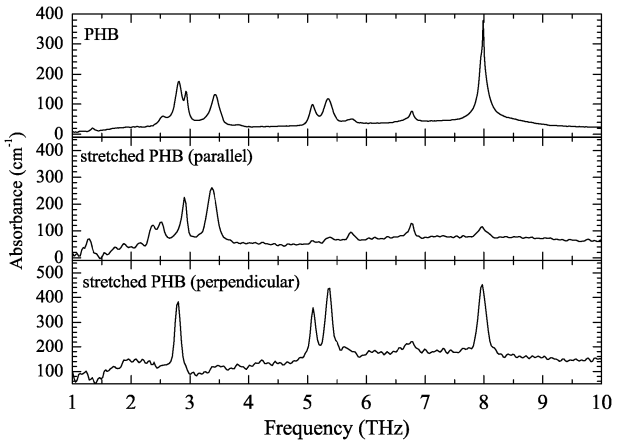

Fig. 3 THz absorption spectra of PHB and polarized THz absorption spectra of highly stretched PHB in the frequency region from 1 to 10 THz, measured by FT-FIR at 10 K. The angle between the stretched direction and the direction of the THz electric field was set to 0° (parallel) and 90° (perpendicular).

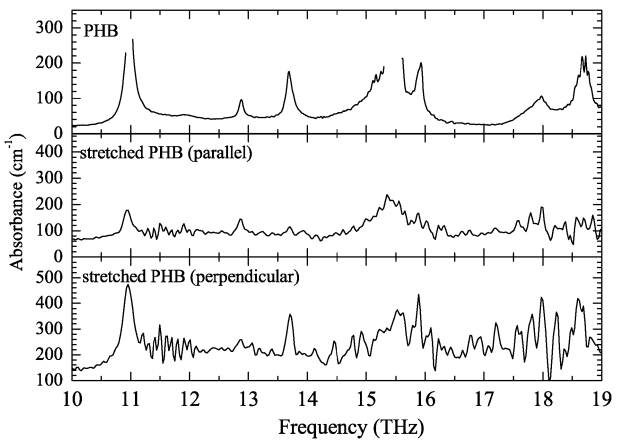

Fig. 4 THz absorption spectra of PHB and polarized THz absorption spectra of highly stretched PHB in the frequency region from 10 to 19 THz, measured by FT-FIR at 10 K. The angle between the stretched direction and the direction of the THz electric field was set to 0° (parallel) and 90° (perpendicular).

Fig. 3 and 4 show absorption spectra of PHB and polarization spectra of stretched PHB measured at 10 K in the 1–10 THz frequency range and in the 10–19 THz range, respectively. In the middle and bottom traces, respectively, the THz electric field was polarized parallel and perpendicular to the stretched direction, which corresponds to the direction of the *c*-axis of the lamellar crystal. The frequencies at 10 K, heights, and polarization properties of peaks in the spectra in Fig. 3 and 4 are summarized in Table 1.

Fig. 3 clearly shows that the peaks at 2.55, 2.93, and 3.43 THz completely disappear in the perpendicularly polarized spectrum, which means that the vibrational transition moments of those peaks are parallel to the *c*-axis of the lamellar crystal. In the lamellar crystal of PHB, C–H···O=C hydrogen bonds are oriented perpendicular to the *c*-axis; see Fig. 1(d). Therefore, we can speculate that those transitions do not originate from the hydrogen bonds. Most probably, those transitions are due to the skeletal vibrations of helical structures. The other transitions are observed in the perpendicular spectrum, which suggests a possible contribution of hydrogen bonding to the vibrational potential.

Table 1 Frequency at 10 K, absorbance peak height, polarization of the transition dipole moment, and temperature shift of the peak frequency of PHB. '//' and '⊥' represent polarization of the vibrational dipole moment parallel and perpendicular to the *c*-axis of the lamellar crystal, respectively. '0' indicates that no clear difference in peak intensity was observed in the polarization spectra

Frequency/THz	Peak height/cm^{-1}	Polarization	Temperature shift/GHz K^{-1}
1.34	20	//	+0.7
2.55	60	//	
2.82	180	⊥	−1.1
2.93	140	//	
3.43	130	//	−1.3
3.82	30	⊥	
5.08	100	⊥	+1.0
5.35	120	⊥	
5.76	50	//	+0.5
6.78	80	//	−0.5
7.98	>300	⊥	
10.98	>300	0	
11.91	60		
12.88	100	//	
13.69	180	⊥	+0.3
15.4	>300	0	
15.93	200	⊥	
17.97	110		
18.7	220	⊥	

Temperature dependence of THz spectra

Fig. 5–8 display temperature-dependent THz absorption spectra of PHB. The spectra in Fig. 5–8 were measured by FT-FIR, and those in Fig. 6 were obtained by THz-TDS. Note that as the temperature increases, the linewidths increase, and some of the peaks shift. Owing to the broadening of the linewidths, couples of vibrational transitions overlap in the absorption bands at higher temperature. For example, four peaks were observed at 10 K between 2.3 and 3.6 THz. The peak at 2.82 THz shifts to lower frequencies as the temperature increases, while that at 2.55 THz does not shift. Both lines are broadened and overlap above 100 K. Also, the peak at 3.43 THz shifts and is merged with the peak at 2.93 THz, which does not shift. Therefore, the two bands at 2.5 THz and 2.9 THz observed in Fig. 6 consist of four transitions, which change the spectral features at higher temperatures. It is necessary to trace the vibrational frequencies at lower frequencies to understand THz absorption spectra measured at higher temperatures. Fig. 9 and 10 plot the frequencies of peaks observed between 1.2 and 3.6 THz and those between 5.0 and 6.9 THz, respectively, *versus* temperature. The peak at 2.82 THz (at 10 K) starts shifting at 40 K and shifts linearly to lower frequencies. On the other hand, the peak at 1.34 THz (10 K) starts shifting at 10 K and shifts to higher frequencies. Thus, the temperature shifting behaviour is quite different in different transitions. The shifts of the peak positions were fitted by a linear function, and the coefficients of the slope are listed in Table 1.

Shifts in peak position and line broadening have been observed in the vibrational spectra of micro-crystalline organic

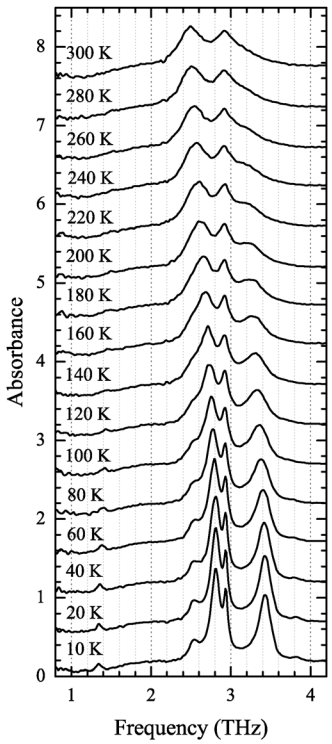

Fig. 5 THz absorption spectra of PHB in the frequency region from 0.8 to 4.2 THz over a temperature range of 10 K to 300 K measured by FT-FIR.

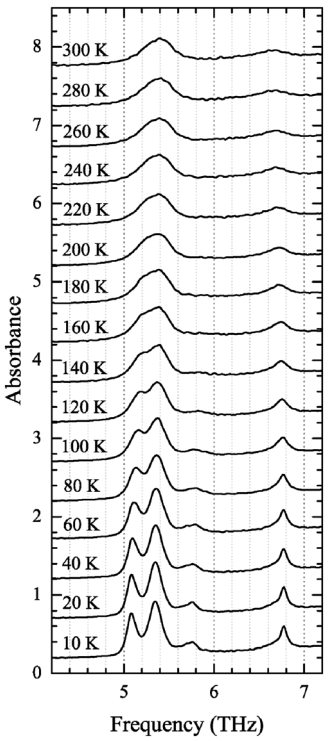

Fig. 7 THz absorption spectra of PHB in the frequency region from 4.2 to 7.2 THz over a temperature range of 10 K to 300 K measured by FT-FIR.

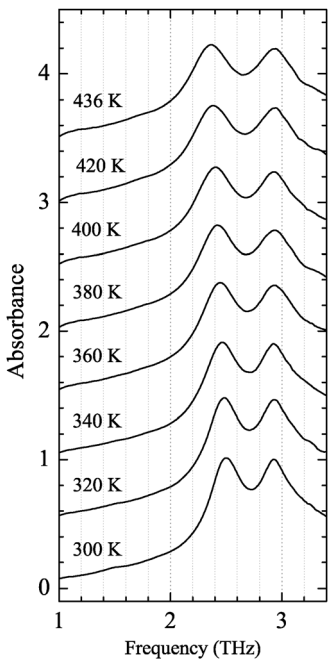

Fig. 6 THz absorption spectra of PHB in the frequency region from 1.0 to 3.4 THz over a temperature range of 300 K to 436 K measured by THz-TDS.

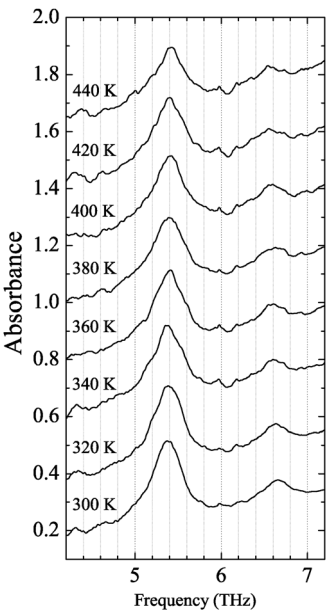

Fig. 8 THz absorption spectra of PHB in the frequency region from 4.2 to 7.2 THz over a temperature range of 300 K to 440 K measured by FT-FIR.

molecules measured at THz frequencies.[15,23,38] The peak shifts can be attributed to the anharmonicity of the vibrational potentials.[15,23] When an anharmonic potential is assumed, the spacing between vibrational levels changes at higher energies. In a THz vibrational spectrum, hot bands are simultaneously observed because of the thermal distribution. When the vibrational frequency is 2.5 THz, only 33% of molecules occupy the lowest vibrational state at 300 K. As a result, an envelope of transitions from different initial states

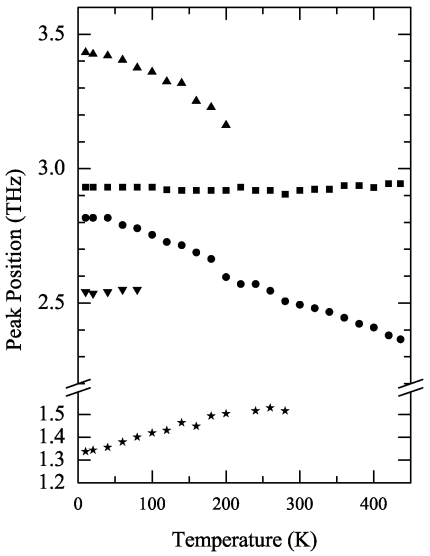

Fig. 9 Peak positions of the THz absorption spectra of PHB in the range of 3.5–1.2 THz *versus* temperature.

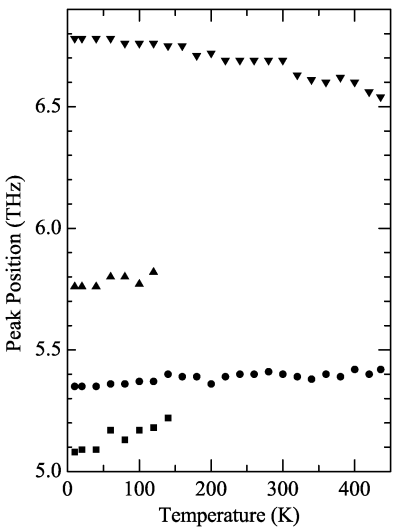

Fig. 10 Peak positions of the THz absorption spectra of PHB in the range of 7.0–5.0 THz *versus* temperature.

makes an inhomogeneous line shape, which changes with the temperature. If the anharmonicity of the vibrational potential is large, the observed transitions show broad, asymmetric line shapes. In Fig. 5, the peak at 3.4 THz, which has a large temperature shift, shows an asymmetric line shape at 10 K, and its left shoulder rises with temperature, indicating a large anharmonicity of the vibrational potential.

Table 1 shows that the temperature shift of the vibrational frequency is quite different for the different transitions. Fig. 9 and 10 show that the curvatures of frequency shifts also differ. However, the frequency shift tends to become larger at lower frequencies. The large anharmonicity at lower frequencies suggests that the vibrational potential is shallow and the vibrational amplitude is large. Those vibrations are probably due to intermolecular interactions, such as hydrogen bonding. On the other hand, most of the peaks above 10 THz show no

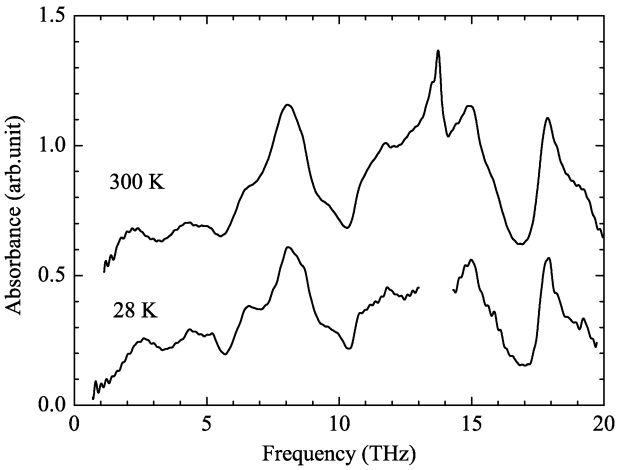

Fig. 11 THz absorption spectra of amorphous PHB measured at 28 K and 300 K by FT-FIR.

frequency shift. The vibrational potential of those peaks may originate from deeper potentials. It is interesting that both negative and positive frequency shifts are observed. When a Lennard–Jones-type potential, which is conventionally used for the calculation of hydrogen bonds, is assumed, the peak shifts must take negative values.[39] The existence of positive peak shifts suggests that such a simple anharmonic potential cannot work when calculating vibrational transition frequencies in the THz frequency region.

Fig. 11 shows THz absorption spectra of amorphous PHB measured at 28 K and 300 K. The glass transition temperature of PHB is about 3 °C.[25] THz time-domain spectra of high-density polyethylene[18,19] and polyvinylidene[19] were recently measured by THz-TDS at different temperatures. The glass transition was observed as a change in the temperature shift in the absorption peak of crystal lattice modes. This research reported a change in the amorphous structure *via* frequency shifts in the lattice vibrational mode. However, no obvious change was observed in the absorption spectra of amorphous PHB measured above and below the glass transition temperature. Also, in Fig. 9 and 10, the peak frequencies shift continuously around the glass transition temperature. Thus, the shape of the PHB absorption spectra does not represent an obvious glass transition.

Conclusion

In this paper, temperature-dependent THz absorption spectra of PHAs with different higher-order conformations, measured by using both THz-TDS and FT-FIR spectrometers, were reported. Clear differences were observed between the spectra of crystalline and amorphous PHB, which shows that the higher-order conformation of PHB determines the THz spectra. The spectrum of P(HB-*co*-HHx) is slightly different from that of PHB, reflecting the difference in the crystallinity and the thickness of the crystal lamellae. The polarization spectra were measured for a stretched PHB sample at 10 K, and the direction of the vibrational transition moment was determined.

The temperature dependences of the spectra revealed that peaks at lower frequencies shift with temperature, suggesting a

large anharmonicity of the vibrational potential. The temperature shifting behaviour is quite different in each transition. Some of the transitions show blue shifts, which cannot be explained by a simple anharmonic potential model. The vibrational dipole transition moment and anharmonicity of the vibrational potential thus obtained should provide important information for the theoretical calculation and assignment of spectra in future.

Acknowledgements

The authors are grateful to Prof. Tadahisa Iwata for the donation of stretched PHB. The authors also thank Mrs Aya Hayashi and Mr Akitsugu Kamiya for their help in the spectral measurement of the samples. This work was supported by Grants-in-Aid for Scientific Research in Japan (KAKENHI 20750067, 22360011).

References

1 P. R. Griffiths, *Far-infrared Spectroscopy*, John Wiley & Sons Inc., Chichester, 2002.
2 P. R. Griffiths and J. A. de Haseth, *Fourier Transform Infrared Spectrometry*, John Wiley & Sons. Inc., New Jersey, 2nd edn, 2007.
3 M. Tonouchi, *Nat. Photonics*, 2007, **1**, 97–105.
4 Y.-S. Lee, *Principles of Terahertz Science and Technology*, Springer, New York, 2009.
5 P. Y. Han, M. Tani, M. Usami, S. Kono, R. Kersting and X. C. Zhang, *J. Appl. Phys.*, 2001, **89**, 2357–2359.
6 K. Kawase, Y. Ogawa and Y. Watanabe, *Opt. Express*, 2003, **11**, 2549–2554.
7 H. Hoshina, Y. Sasaki, A. Hayashi, C. Otani and K. Kawase, *Appl. Spectrosc.*, 2009, **63**, 81–86.
8 K. Yamamoto, M. Yamaguchi, F. Miyamaru, M. Tani, M. Hangyo, T. Ikeda, A. Matsushita, K. Koide, M. Tatsuno and Y. Minami, *Jpn. J. Appl. Phys.*, 2004, **43**, L414–L417.
9 W. H. Fan, A. Burnett, P. C. Upadhya, J. Cunningham, E. H. Linfield and A. G. Davies, *Appl. Spectrosc.*, 2007, **61**, 638–643.
10 K. Fukunaga, Y. Ogawa, S. Hayashi and I. Hosako, *IEICE Electron. Express*, 2007, **4**, 258–263.
11 A. G. Davies, A. D. Burnett, W. H. Fan, E. H. Linfield and J. E. Cunningham, *Mater. Today*, 2008, **11**, 18–26.
12 B. Ferguson and X. C. Zhang, *Nat. Mater.*, 2002, **1**, 26–33.
13 M. Walther, B. M. Fischer and P. U. Jepsen, *Chem. Phys.*, 2003, **288**, 261–268.
14 P. U. Jepsen and S. J. Clark, *Chem. Phys. Lett.*, 2007, **442**, 275–280.
15 M. D. King, W. D. Buchanan and T. M. Korter, *J. Phys. Chem. A*, 2010, **114**, 9570–9578.
16 H. Hoshina, Y. Morisawa, H. Sato, A. Kamiya, I. Noda, Y. Ozaki and C. Otani, *Appl. Phys. Lett.*, 2010, **96**, 101904.
17 V. A. Bershtein and V. A. Ryzhov, *Adv. Polym. Sci.*, 1994, **114**, 43–121.
18 S. Wietzke, C. Jansen, T. Jung, M. Reuter, B. Baudrit, M. Bastian, S. Chatterjee and M. Koch, *Opt. Express*, 2009, **17**, 19006–19014.
19 S. Wietzke, C. Jansen, M. Reuter, T. Jung, J. Hehl, D. Kraft, S. Chatterjee, A. Greiner and M. Koch, *Appl. Phys. Lett.*, 2010, **97**, 022901.
20 W. F. X. Frank and H. Fiedler, *Infrared Phys.*, 1979, **19**, 481–489.
21 D. Y. Shen, S. K. Pollack and S. L. Hsu, *Macromolecules*, 1989, **22**, 2564–2569.
22 M. Fuse, R. Sato, M. Mizuno, K. Fukunaga, K. Itoh and Y. Ohki, *Jpn. J. Appl. Phys.*, 2010, **49**, 102402.
23 Y. C. Shen, P. C. Upadhya, E. H. Linfield and A. G. Davies, *Appl. Phys. Lett.*, 2003, **82**, 2350–2352.
24 I. Noda, R. H. Marchessault and M. Terada, *Polymer Data Handbook*, Oxford University Press, Oxford, 2009.
25 I. Noda, S. B. Lindsey and D. Caraway, *Microbiology Monographs*, 2010, **14**, 237–255.
26 M. Kunioka, A. Tamaki and Y. Doi, *Macromolecules*, 1989, **22**, 694–697.
27 Y. Doi, S. Kitamura and H. Abe, *Macromolecules*, 1995, **28**, 4822–4828.
28 H. Abe, Y. Doi, H. Aoki and T. Akehata, *Macromolecules*, 1998, **31**, 1791–1797.
29 T. Iwata, Y. Aoyagi, T. Tanaka, M. Fujita, A. Takeuchi, Y. Suzuki and K. Uesugi, *Macromolecules*, 2006, **39**, 5789–5795.
30 M. Yokouchi, Y. Chatani, H. Tadokoro, K. Teranishi and H. Tani, *Polymer*, 1973, **14**, 267–272.
31 H. Sato, R. Murakami, A. Padermshoke, F. Hirose, K. Senda, I. Noda and Y. Ozaki, *Macromolecules*, 2004, **37**, 7203–7213.
32 H. Sato, Y. Ando, J. Dybal, T. Iwata, I. Noda and Y. Ozaki, *Macromolecules*, 2008, **41**, 4305–4312.
33 H. Sato, K. Mori, R. Murakami, Y. Ando, I. Takahashi, J. M. Zhang, H. Terauchi, F. Hirose, K. Senda, K. Tashiro, I. Noda and Y. Ozaki, *Macromolecules*, 2006, **39**, 1525–1531.
34 H. Sato, R. Murakami, J. M. Zhang, Y. Ozaki, K. Mori, I. Takahashi, H. Terauchi and I. Noda, *Macromol. Res.*, 2006, **14**, 408–415.
35 R. Murakami, H. Sato, J. Dybal, T. Iwata and Y. Ozaki, *Polymer*, 2007, **48**, 2672–2680.
36 Y. Hu, J. M. Zhang, H. Sato, Y. Futami, I. Noda and Y. Ozaki, *Macromolecules*, 2006, **39**, 3841–3847.
37 H. Sato, M. Nakamura, A. Padermshoke, H. Yamaguchi, H. Terauchi, S. Ekgasit, I. Noda and Y. Ozaki, *Macromolecules*, 2004, **37**, 3763–3769.
38 In THz database http://www.riken.jp/THzdatabase/.
39 P. F. Bernath, *Spectra of Atoms and Molecules*, Oxford University Press, New York, 2005.